The catalytic enantioselective [1,2]-Wittig rearrangement cascade of allylic ethers

Tengfei Kang,[1,2] Justin O'Yang,[1] Kevin Kasten,[1] Samuel S. Allsop,[3] Toby Lewis-Atwell,[3,4] Elliot H. E. Farrar,[3] Martin Juhl,[1] David B. Cordes,[1] Aidan P. McKay,[1] Matthew N. Grayson,[3*] Andrew D. Smith[1*]

[1] EaStCHEM, School of Chemistry, University of St Andrews, North Haugh, St Andrews, KY16 9ST, UK.

[2] Key Laboratory of Applied Surface and Colloid Chemistry, Ministry of Education, and School of Chemistry and Chemical Engineering, Shaanxi Normal University, Xi'an, Shaanxi, China, 710119.

[3] Department of Chemistry, University of Bath, Claverton Down, Bath, BA2 7AY, UK.

[4] Department of Computer Science, University of Bath, Claverton Down, Bath, BA2 7AY, UK.

*e-mail: ads10@st-andrews.ac.uk; M.N.Grayson@bath.ac.uk

Abstract

The catalytic enantioselective [1,2]-Wittig rearrangement of allylic ethers constitutes a recognised synthetic challenge as it is traditionally considered to arise from a non-concerted reaction pathway *via* formation and recombination of radical pairs. Here we show a catalytic enantioselective solution to this challenge, demonstrating that [1,2]-Wittig products are generated *via* an alternative reaction cascade to traditional dogma. The developed process employs a chiral bifunctional iminophosphorane (BIMP) catalyst to promote an initial enantioselective [2,3]-sigmatropic rearrangement. A subsequent base promoted, stereoconvergent, fragmentation-recombination process that proceeds with high enantiospecificity and retention of configuration, formally equivalent to a Woodward-Hoffmann forbidden thermal [1,3]-sigmatropic rearrangement, generates [1,2]-Wittig products in up to 97:3 e.r. Supported by extensive DFT calculations, this chirality transfer process will have broad implications for fundamental stereocontrol in organic transformations.

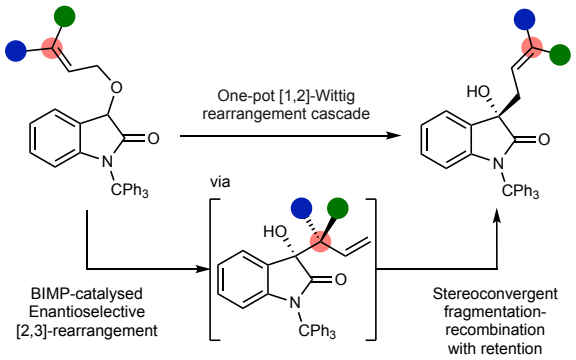

The catalytic enantioselective [1,2]-Wittig rearrangement cascade of allylic ethers

Tengfei Kang,[1,2] Justin O'Yang,[1] Kevin Kasten,[1] Samuel S. Allsop,[3] Toby Lewis-Atwell,[3,4] Elliot H. E. Farrar,[3] Martin Juhl,[1] David B. Cordes,[1] Aidan P. McKay,[1] Matthew N. Grayson,[3*] Andrew D. Smith[1*]

[1] EaStCHEM, School of Chemistry, University of St Andrews, North Haugh, St Andrews, KY16 9ST, UK.

[2] Key Laboratory of Applied Surface and Colloid Chemistry, Ministry of Education, and School of Chemistry and Chemical Engineering, Shaanxi Normal University, Xi'an, Shaanxi, China, 710119.

[3] Department of Chemistry, University of Bath, Claverton Down, Bath, BA2 7AY, UK.

[4] Department of Computer Science, University of Bath, Claverton Down, Bath, BA2 7AY, UK.

*e-mail: ads10@st-andrews.ac.uk; M.N.Grayson@bath.ac.uk

Abstract

The catalytic enantioselective [1,2]-Wittig rearrangement of allylic ethers constitutes a recognised synthetic challenge as it is traditionally considered to arise from a non-concerted reaction pathway *via* formation and recombination of radical pairs. Here we show a catalytic enantioselective solution to this challenge, demonstrating that [1,2]-Wittig products are generated *via* an alternative reaction cascade to traditional dogma. The developed process employs a chiral bifunctional iminophosphorane (BIMP) catalyst to promote an initial enantioselective [2,3]-sigmatropic rearrangement. A subsequent base promoted, stereoconvergent, fragmentation-recombination process that proceeds with high enantiospecificity and retention of configuration, formally equivalent to a Woodward-Hoffmann forbidden thermal [1,3]-sigmatropic rearrangement, generates [1,2]-Wittig products in up to 97:3 e.r. Supported by extensive DFT calculations, this chirality transfer process will have broad implications for fundamental stereocontrol in organic transformations.

Main text:

Sigmatropic rearrangements are useful and reliable atom-economic reactions, with their ability to form carbon-carbon and carbon-heteroatom bonds through well-defined and predictable transition states[1] making these processes attractive for the synthesis of complex targets[2]. Among this broad set of reaction processes, [2,3]- and [1,2]-sigmatropic rearrangements are of synthetic and mechanistic significance[3,4]. The rearrangement of allylic ethers under basic reaction conditions typically leads to product mixtures proposed to arise from the thermally allowed concerted [2,3]-sigmatropic Wittig rearrangement, alongside a competitive non-concerted [1,2]-Wittig rearrangement generally thought to arise from homolytic fragmentation of the anionic intermediate to form a geminate radical pair and their subsequent recombination (Figure 1A) [5,6]. As representative examples, both Rautenstrauch [7] and Baldwin [8] have shown that treatment of benzyl allyl ether **1** with *n*BuLi gives rise to a mixture of [2,3]- and [1,2]-products **2** and **3**, respectively, with increased [1,2]-product observed at higher temperatures. Although not widely recognised, sporadic control reactions have demonstrated the feasibility of converting [2,3]-Wittig products to [1,2]-Wittig products (formally *via* a [1,3]-rearrangement), although the generality, mechanism and configurational consequence has not been established [9-15]. The concerted or dissociative (*via* ionic or radical intermediates) nature of both the [1,2]- and [1,3]-processes has been much debated. For example, Danheiser considered a concerted [1,3]-pathway to account for the inversion observed in the ring expansion of *cis*-cyclobutanol **4** [16]. However, Gajewski [17] and Cohen [18] both postulated a nonconcerted fragmentation pathway *via* an intermediate allylic anion that accounts for the observed *in situ* isomerism of *cis*-**4** to *trans*-**6**, and that use of enantiomerically pure *cis*-**4** or *trans*-**6** leads to racemic product **5** (Figure 1B) [19]. Applying the Woodward-Hoffmann rules indicates that a concerted [1,2]-rearrangement is forbidden, while a thermal [1,3]-rearrangement is symmetry allowed but geometrically challenging, with a suprafacial carbon shift expected to proceed with inversion of configuration at the oxygen bearing carbon[1]. Interestingly, Houk has previously shown that anionic Cope and amino-Cope reactions proceed through a stepwise dissociation-recombination process [20], consistent with competitive non-concerted [1,3]-rearrangements observed in related systems [21,22]. Given the mechanistic ambiguity surrounding these processes the enantioselective [1,2]-Wittig rearrangement of allylic ethers is a recognised challenge and is currently unknown despite its synthetic potential [23].

In this manuscript, the catalytic enantioselective [1,2]-Wittig rearrangement of allylic ethers is developed (up to 97:3 e.r.) and is shown to proceed through a cascade process consisting of an initial enantioselective [2,3]-rearrangement (up to >99:1 e.r.) promoted by a bifunctional iminophosphorane (BIMP) catalyst. The resultant tertiary carbinol bearing an α-branched allylic substituent is transformed to the linear [1,2]-Wittig isomeric product with retention of configuration at the oxygen bearing carbon (equivalent to a Woodward-Hoffmann forbidden [1,3]-sigmatropic rearrangement) through a dissociative intramolecular fragmentation-recombination event with high enantiospecificity (Figure 1C). Substitution reactions that proceed with retention of configuration are rare, although recognised for alcohols *via* an S_Ni mechanism that proceed *via* contact ion-paired intermediates [24-26]. Traditionally the stereospecificity of nucleophilic substitution processes leads to inversion of configuration in S_N2 reaction processes at secondary centres and partial or complete racemisation in S_N1 processes at tertiary centres. However recent advances have showcased stereospecific substitution at tertiary and even quaternary centres in which stereochemical information is conferred despite ionization of a substrate [27-32]. In this context, the high enantiospecificity of the observed chirality transfer protocol that leads to [1,2]-products with retention of configuration, while proceeding through an ionic fragmentation and recombination process, is significant and holds promise for the elucidation of alternative reaction pathways for generating chiral products with high enantioselectivity.

Reaction Development

Building upon the observation that disubstitution at the allylic ether terminus typically leads to increased preference for [1,2]-rearrangement products [14], the use of bifunctional iminophosphoranes (BIMPs) as organocatalysts to promote the enantioselective [1,2]-rearrangement process was considered. Originally developed by Dixon, BIMPs have shown widespread use in a plethora of stereoselective transformations [33], possessing a Brønsted superbasic iminophosphorane with an H-bond donor to assert stereocontrol. Rearrangement of an allylic ether upon an oxindole skeleton was chosen given the prevalence of this motif in natural products and bioactive molecules, as well as expected acidity. Following initial screening of the effect of *N*-substituent (*N*-Me, *N*-Bn, *N*-trityl), BIMP catalyst, solvent and temperature variation (see Supplementary Information section 2) using *N*-trityl substituted allylic ether **8** and *t*Bu-BIMP catalyst **7** showed that rearrangement to **9** in mesitylene led to selective formation of the [1,2]-product in excellent yield and promising enantioselectivity after 24 hours (Figure 2A, 92:8 e.r.). As [1,2]-Wittig products are traditionally expected to be generated *via* a radical recombination mechanism the effect of adding 20 mol% of 4-NHAc-TEMPO as an additive was probed. Formation of the [1,2]-product was not significantly inhibited, giving **9** in 73% yield and improved 95:5 e.r., with no 4-NHAc-TEMPO adducts observed [34]. The mass balance consisted of the aldol side product **10** (>95:5 dr, 75:25 e.r.) that was isolated in 5% yield; addition of 1.0 equivalent of 4-NHAc-TEMPO was also tested, affording **9** in a further reduced 59% yield but enhanced 97:3 e.r. Control experiments indicated that taking a 1:1 mixture of allylic ether **8** and *N*-tritylisatin with *t*Bu-BIMP **7** gave aldol product **10** in 71% yield (>95:5 dr, 75:25 e.r.), consistent with *in situ* formation of *N*-tritylisatin derivative in the presence of 4-NHAc-TEMPO. Further experiments showed that addition of 1.0 equivalent of TEMPO led to **9** in 57% isolated yield (97:3 e.r.) with 10% of TEMPO-allyl adduct (**T-a**) isolated as well as 11% *N*-tritylisatin. Intrigued by these observations, *in situ* temporal reaction analysis monitored consumption of allylic ether **11** (40 mM) upon treatment with *t*Bu-BIMP **7** (20 mol%) to give [1,2]-Wittig product **13** in d_8-toluene using ^{1}H NMR spectroscopy (Figure 2B; see Supplementary Information section 5.1). The rearrangement showed a first-order consumption in substrate **11** (that was racemic throughout the reaction process), with a transient mixture of diastereoisomeric [2,3]-rearrangement products **12** detected (δ_H = 5.15 and 4.87 ppm) that accumulated to a maximum concentration of ≈ 15 mM and was subsequently transformed into the [1,2]-rearrangement product **13**, consistent with **12** being an intermediate in the generation of **13**. On a synthetic scale, stopping the reaction of allylic ether **8** after 1 h gave, at 75% conversion, a 63:37 mixture of [2,3]-products **14** and [1,2]-product **9** (96:4 e.r.). Purification gave **14** (89:11 dr, both diastereoisomers 99:1 e.r.) in 21% yield whose absolute configuration was determined by *N*-trityl deprotection and subsequent single crystal X-ray diffraction (see Supplementary Information section 6). The absolute configuration within **9** was confirmed by chemical synthesis (see Supplementary Information section 8.8), indicating stereoconvergence and retention of configuration at C(3) in the rearrangement of diastereoisomers **14** to **9**. Separate control experiments validated the [2,3]-rearrangement products **14** as intermediates to the [1,2]-product **9** (Figure 2C). Treating **14** (89:11 dr) with *t*Bu-BIMP **7** and 4-NHAc-TEMPO for 5 h gave the [1,2]-product **9** in 60% yield

(99:1 e.r.) alongside 10% of *N*-tritylisatin, while treatment with *t*Bu-BIMP **7** and TEMPO gave the [1,2]-product **9** in 43% yield (97:3 e.r.) alongside 12% of TEMPO-adduct (**T-a**) and 15% of *N*-tritylisatin. Treatment with *t*Bu-BIMP **7** alone gave **9** in 83% yield (96:4 e.r.) with 12% of *N*-tritylisatin observed, while the use of achiral base DBU upon **14** also promoted rearrangement, but to moderate 50% conversion, giving **9** in 36% yield but with high enantioselectivity (96:4 e.r.). This is consistent with DBU or *t*Bu-BIMP **7** acting as a base and not significantly influencing enantiospecificity in this [1,3]-rearrangement process. Consistent with this observation, monitoring the conversion of **14** (89:11 dr) to **9** upon treatment with racemic or enantiopure BIMP derivatives did not lead to significant rate differences (see Supplementary Information section 5.2) implying no matched and mismatched reactant combinations. Taken together these experiments are consistent with the addition of 4-NHAc-TEMPO or TEMPO leading to enhanced enantiospecificity in the base promoted stereoconvergent [1,3]-rearrangement. This is consistent with selective fragment trapping within this process leading to enhanced selectivity, with the origin of this phenomenon discussed in the Mechanistic Analysis section. The [2,3]-product **14** could also be transformed into the [1,2]-Wittig product **9** when heated at 100 °C without the addition of base, albeit with reduced yield (31%) and enantioselectivity (92:8 e.r.). Crossover experiments (Figure 2D) using a 50:50 mixture of ethers **15** and **16** either with *t*Bu-BIMP **7** alone (conditions a), or with the addition of 4-NHAc-TEMPO (conditions b), resulted in only [1,2]-products **17** and **18**, consistent with an intramolecular process in operation, with enhanced product enantioselectivity again observed in the presence of 4-NHAc-TEMPO.

Having identified a viable reaction pathway, the scope of the enantioselective [1,2]-Wittig cascade was examined (Table 1). Changing the C(3')-alkyl substituent from methyl- to ethyl- was tolerated giving **19**, while using a C(3')-cyclopropyl substituted allylic ether as a radical probe generated only [1,2]-rearrangement product **20** (40% yield, 96:4 e.r.) with the cyclopropyl ring intact. Although indicative, the absence of ring-opened products does not exclude a radical mechanism since in cage carbon-carbon radical recombination (rate constant typically estimated to be $>10^{11}$ s−1) is considered much faster than ring-opening of a cyclopropyl methyl radical ($k = 1.3 \times 10^{8}$ s–1)[35]. Increasing the steric hindrance through incorporation of a C(3')-phenyl substituent resulted in moderate conversion (see Supplementary Information section 4). This necessitated changing the *N*-trityl substituent to an *N*-benzyl for increased reactivity, giving **21** in 61% yield but reduced product enantioselectivity (73:27 e.r.), consistent with screening studies that necessitated *N*-trityl substitution for optimal enantioselectivity (see Supplementary Information section 2). A limitation of this process showed that both a (*Z*)-configured allylic ether and a dimethyl terminal allylic ether returned only starting material under the reaction conditions. Variation of the C(3')-aryl substituent showed that the incorporation of halogens (4-F, 4-Cl and 4-Br), electron withdrawing (4-CF_3), as well as electron-donating (4-Ph, 4-Me, 4-MeO) substituents were tolerated, giving the [1,2]-rearrangement products **13**, **18**, **22-26** in high yields and enantioselectivity. The incorporation of 3-Me- and 2-Me substituents (**27**, **28**) was also tolerated, although with lower yields for the 2-Me-substituted example. In addition, 2-naphthyl, thien-2-yl and thiazol-2-yl-substituted ethers all afforded the corresponding [1,2]-Wittig products **29-31** in 71% to 82% yields with 93:7 to 94:6 e.r. Substituent variation within the 4-, 5- and 6-positions of the oxindole included the incorporation of halogen (5-F, 5-Cl, 5-I, 6-Br, 6-Cl), electron-withdrawing (5-O_2N) and electron-donating (5-Me, 5-MeO) substituents that gave the corresponding products **17**, **32-39** in 67% to 80% yield and up to 96:4 e.r. While *N*-tritylation of 7-chloroisatin was unsuccessful, the *N*-benzyl analogue was prepared and tested, giving **40** in 81% yield but reduced enantioselectivity (73:27 e.r.).

To further probe the generality of this transformation, the effect of incorporating C(3')-F or C(3')-H substituents within the allylic ether terminus was investigated (Figure 3A). In contrast to the parent C(3')-methyl series, treatment of **41** and **43** with *t*Bu-BIMP **7** at room temperature gave exclusively the corresponding [2,3]-rearrangement products **42** (91:9 dr, 98:2 e.r.) and **44** (72:28 dr, 98:2 e.r.) with no formation of the [1,2]-product. To convert these enantioenriched [2,3]-products to the corresponding [1,2]-Wittig products increased reaction temperatures (≥100 ˚C for **42** and **44**) and the addition of stoichiometric DBU (1 equiv.) was required. For example, stereoconvergence of the separable diastereoisomers (3*S*,1'*S*)- and (3*S*,1'*R*)-**44** upon treatment with DBU in mesitylene at 120 ˚C was observed, with both giving (*E*,*S*)-[1,2]-Wittig product **45** in 94:6 and 93:7 e.r., respectively. Solvent polarity has a significant effect upon the enantiospecificity of the [1,3]-rearrangement at these increased reaction temperatures (see Supplementary Information section 3) with highest product enantioselectivity observed in solvents of low polarity (toluene

and mesitylene) rather than polar solvents (DMF or MeCN). Rearrangement with retention of configuration is still observed, although addition of 4-NHAc-TEMPO or TEMPO does not lead to increased product e.r. in this series (see Supplementary Information section 3). Having demonstrated that high temperatures are required to promote the [1,3]-rearrangement of the initially formed [2,3]-products, a telescoped process to allow one-pot access to [1,2]-Wittig products was developed that utilised toluene as a solvent (Figure 3B). Treatment of a range of allylic ethers with *t*Bu-BIMP **7** promoted enantioselective [2,3]-rearrangement, that was followed by the addition of DBU (1 equiv.) and heating to between 60 ˚C and 100 ˚C. Following this procedure, in the C(3')-F series, inclusion of Ph, 4-MeC_6H_4, 4-$MeOC_6H_4$ and 4-$F_3CC_6H_4$-substituted allylic ethers, as well as 4-Cl, 5-F, 5-NO_2, 5-MeO and 6-Cl substituents within the oxindole were tolerated, giving the corresponding [1,2]-Wittig products (**46**-**54**) with good to excellent enantioselectivity (91:9 to 97:3 e.r.). In the C(3')-H series, variation of the aryl substituent within the allylic ether showed that Ph, 4-$MeOC_6H_4$, 4-$F_3CC_6H_4$, 4-FC_6H_4, 2-$MeOC_6H_4$, 1-naphthyl and 2-naphthyl-substitution, heteroaromatic 3-thienyl and C(2')-methyl substitution, alongside 4-Cl, 5-OMe and 6-Br substituents within the oxindole were tolerated, allowing the formation of enantioenriched [1,2]-Wittig rearrangement products **45, 55**-**65** (87:13 to 95:5 e.r.). Notably, lower product yields (41% to 73%) were observed in this one-pot process than noted in Figure 3, reflecting the propensity for competitive decomposition at the elevated reaction temperatures required to promote the [1,3]-rearrangement.

Mechanistic Analysis

Having demonstrated the scope of this transformation, consideration to the mechanism of this cascade was given. Initial association of *t*Bu-BIMP **7** to substrate **I** by hydrogen-bonding is assumed to direct deprotonation of the allylic ether-BIMP complex **II** to give **III**, with subsequent concerted [2,3]-sigmatropic rearrangement giving **IV** with high stereoselectivity (Figure 4A). Protonation and catalyst release gives isolable **V**. A subsequent base (*t*Bu-BIMP or DBU) promoted anion-accelerated [1,3]-rearrangement from **IV**[36], that proceeds with retention of configuration at the carbinol centre, generates [1,2]-Wittig product **VI**. Computational methods were used to gain mechanistic insight into the [2,3]- and [1,3]-rearrangement processes. Eight binding modes between [*t*Bu-BIMP-H]$^+$ and the substrate were considered (see Supplementary Information Figure S19) and conformationally searched using CREST (GFN2-xTB; Ar = Ph, X = Me)[37-39]. The lowest energy conformer from each search was then optimised in Gaussian 16[40] using ONIOM[41,42] to reduce the computational complexity for this large system. The peripheral components of both catalyst and substrate were treated with semiempirical quantum mechanics (SQM) and placed in the low layer, while the atoms involved in bond breaking and forming were treated with DFT. Full DFT single point energies were performed on all stationary points (see Supplementary Information section 7). These calculations were conducted on substrate **8** (Ar = Ph, X = Me, Figure 4A) in the presence of catalyst **7** unless otherwise stated (Figure 2C). Previous studies have shown that there is good agreement between ONIOM and full DFT calculations for other organocatalytic systems[43-49].

[2,3]-Sigmatropic Rearrangement

To study the origins of stereoselectivity, TSs leading to each of the four possible stereoisomers for the BIMP-catalysed [2,3]-sigmatropic rearrangement were located (Ar = Ph, X = Me). Consistent with experimental results (Figure 2C), the calculated lowest energy *exo*-TS forms the (*S*,*S*)-stereoisomer, with the difference in free energy between this and the lowest energy *exo*-(*R*,*R*)-TS (1.57 kcal mol^{-1}, Figure 4B) resulting in a computed e.r. of 93:7[50]. The diastereomeric ratio computed from the ***exo*-(*S*,*S*)-** and ***endo*-(*S*,*R*)-TS III** energies ($\Delta\Delta G^{\ddagger}$ = 1.16 kcal mol^{-1}) is 86:14. These ratios are consistent with the experimentally observed levels of stereoselectivity in the [2,3]-sigmatropic rearrangement. To gain insight into the origins of enantioselectivity, the structures of ***exo*-(*S*,*S*)-** and ***exo*-(*R*,*R*)-TS III** were compared, revealing key differences in hydrogen bonding capability between [*t*Bu-BIMP-H]$^+$ and the substrate. In ***exo*-(*S*,*S*)-TS III**, three stabilising NH···O hydrogen bonds from the catalyst to the substrate oxygen atoms are observed, while in ***exo*-(*R*,*R*)-TS III**, only two NH···O hydrogen bonds are seen alongside an unusual, longer and weaker NH···C interaction with a reacting carbon atom (see Figure 4B and Supplementary Information Figure S21). The origins of diastereoselectivity can be understood by comparison of ***exo*-(*S*,*S*)-TS III** and ***endo*-(*S*,*R*)-TS III**. A shorter

distance between the centroids of the allylic aryl substituent and an *N*-trityl Ph substituent in ***exo*-(*S*,*S*)-TS III** (4.74 Å) relative to ***endo*-(*S*,*R*)-TS III** (5.12 Å) is observed, suggesting a more favourable T-shaped π-stacking interaction, leading to the preference for the (*S*,*S*)-stereoisomer[51] (see Figure 4B and Supplementary Information Figure S22).

[1,3]-Rearrangement

Computational analysis subsequently studied the feasibility of a concerted rearrangement or a stepwise fragmentation followed by a recombination process (Figure 4A) for the onwards reaction of **(*S*,*S*)-IV** (Ar = Ph, X = Me). Although examples of [1,3]-sigmatropic rearrangements are reported[52-58], despite extensive efforts it was not possible to locate concerted TSs for this [1,3]-rearrangement process, even with constraints between the bond-forming and bond-breaking atoms; some unconstrained attempts resulted in geometries which resembled **TS IV** (fragmentation). Optimisation of fragmentation TSs was possible but attempts to locate a TS that connects the fragment complex and the recombination product were all unsuccessful. An energy scan starting from the recombination product up to a fragment complex (see Supplementary Information Figure S23) showed no peak in the potential energy surface between 1.6 and 3.5 Å which suggests that **VI** forms via a near barrierless recombination event. Reoptimisation of the lowest energy **(*S*,*S*)-TS IV** conformer with unrestricted methods showed no appreciable spin density on any atom which is consistent with an ionic rather than a homolytic fragmentation.

The lowest energy conformer of **(*S*,*S*)-IV** and **(*S*,*S*)-TS IV** were then reoptimised with Ar = 4-FC_6H_4, X = Me such that the calculated reaction barrier could be directly compared to that derived from *in situ* reaction monitoring (Figure 2B, see Supplementary Information section 7.3). The intrinsic reaction coordinate (IRC) data for the reoptimised 4-FC_6H_4 TS (**(*S*,*S*)-TS IV$_F$**) is shown in Figure 4C (for optimised structures of **(*S*,*S*)-IV$_F$**, **(*S*,*S*)-TS IV$_F$** and fragment complex, see Supplementary Information Figure S24). The computed barrier for the fragmentation step of this [1,3]-rearrangement ($\Delta G^{\ddagger}_{comp}$ = 20.97 kcal mol^{-1}) closely matches that derived from kinetic fitting of the reaction profile generated via *in situ* monitoring of **11→12→13** ($\Delta G^{\ddagger}_{exp}$ = 21.90 kcal mol^{-1}, see Figure 2B and Supplementary Information section 5.4).

To experimentally probe the validity of this proposed fragmentation-recombination pathway, taking isolated racemic [2,3]-rearrangement products that differed in the electronic effect of C(1')-aryl substituents with *t*Bu-BIMP **7** showed that inclusion of electron withdrawing substituents led to enhanced reaction rates. Hammett analysis (Figure 5A; see Supplementary Information section 5.2) revealed a ρ value of +0.76 when plotted against the substituent constant σ−. Although small, this ρ value is consistent with the build-up of partial negative charge within the rate limiting TS of the reaction and the proposed anionic fragmentation. Notably no significant difference in reaction rate was observed when using BIMP catalysts with either racemic or enantioenriched [2,3]-rearrangement products (see Supplementary Information section 5.3). Building upon this observation the effect of incorporating an electron withdrawing ester substituent at C(3') within the allylic ether terminus was investigated (Figure 5B, see Supplementary Information section 3). Treatment of **66** (R^1 = Me) with *t*Bu-BIMP **7** at rt promoted initial enantioselective [2,3]-rearrangement, leading to [1,2]-product **67** in 55% yield (98:2 e.r.) alongside aldol product **68** (15%, 75:25 dr, 88:12 e.r.) and *N*-tritylisatin (7%). Notably treatment of **69** (R^1 = H) with *t*Bu-BIMP **7** at rt for 1 hour, followed by warming at 40 ˚C for 2 hours led to facile fragmentation, giving [1,2]-product **70** in 48% yield (95:5 e.r.) in conjunction with ethyl crotonate (22% yield) and *N*-tritylisatin (26%). The generation of ethyl crotonate **71** and *N*-tritylisatin is consistent with the ester substituent facilitating anionic fragmentation from an initially formed [2,3]-product, with protonation and isomerisation giving **71**. Building on these observations, the observed [1,3]-rearrangement with retention of configuration and high enantiospecificity is consistent with anionic fragmentation from an alkoxide·[*t*Bu-BIMP-H]$^+$ complex generating an intimate ion pair consisting of an allylic anion and *N*-tritylisatin·[*t*Bu-BIMP-H]$^+$ (Figure 4C). Recombination at the terminal allylic position upon the *Re*-face of the isatin occurs at a faster rate than ion pair dissociation, or conformational change and bond rotation, to allow *Si*-face addition of the isatin that would lead to reduced product enantioselectivity. Given this anionic fragmentation-recombination mechanism the observation of improved product enantioselectivity upon addition of TEMPO-derivatives (Figure 2A) is ascribed to initial SET oxidation of an anionic carbanion intermediate by TEMPO as it dissociates from the intimate ion-pair, followed by trapping with a second equivalent of TEMPO, consistent with observations by Studer and co-workers alongside others[59-62]. Alternative mechanisms involving radical

fragmentation and subsequent recombination, or anionic fragmentation and protonation, followed by C-H abstraction by TEMPO and subsequent radical recombination were ruled out (see Supplementary Information section 3).

Summary

To conclude, a cascade process that allows the catalytic enantioselective [1,2]-Wittig rearrangement of allylic ethers has been developed, providing enantioenriched homoallylic tertiary alcohols with high enantioselectivity. Contrary to existing dogma, mechanistic studies and DFT calculations strongly support a cascade mechanism for this process that involves an initial enantioselective [2,3]-rearrangement of the allylic ether catalysed by a chiral *t*Bu-BIMP catalyst. This is followed by a base-promoted anionic fragmentation-recombination pathway (base = *t*Bu-BIMP or DBU), that proceeds with high levels of enantiospecificity even at elevated reaction temperatures. Substitution of the allylic fragment significantly affects the effectiveness of the fragmentation/recombination pathway, with anion stabilising ester substituents facilitating fragmentation, and with C(3')-alkyl substitution leading to enhanced rates of [1,2]-product formation over C(3')-F or C(3')-H substitution. Given the importance of understanding fundamental reaction processes that lead to stereochemical control, the enantiospecificity observed in this non-concerted pathway will have broader implications for a plethora of other related synthetic transformations.

Acknowledgements

The research leading to these results has received funding from the Royal Society (Newton Fellowship to TK), EPSRC (TK, KK, EP/T023643/1; ADS, KK EP/W007517; EHEF, EP/R513155/1; EHEF, MNG, EP/W003724/1), UKRI (TLA, ART-AI CDT, EP/S023437/1), The Carlsberg Foundation (MJ) and the EaSI-CAT centre for Doctoral Training (JOY). The authors gratefully acknowledge the University of Bath's Research Computing Group (doi.org/10.15125/b6cd-s854) for their support in this work.

Author Contributions: ADS conceived the project; TK, KK and ADS designed the synthetic experiments; TK, KK, JOY and MJ carried out all synthetic experimental studies and analysed the reactions. SSA, TL-A and EHEF carried out all computation in consultation with MNG; ADS, TK, SSA, TL-A, EHEF and MNG prepared the manuscript that was agreed by all authors. DBC and APM carried out single crystal X-ray analysis. Correspondence regarding computation should be addressed to MNG; all other correspondence should be addressed to ADS.

Ethics Declaration:
Competing interests:
The authors declare no competing interests.

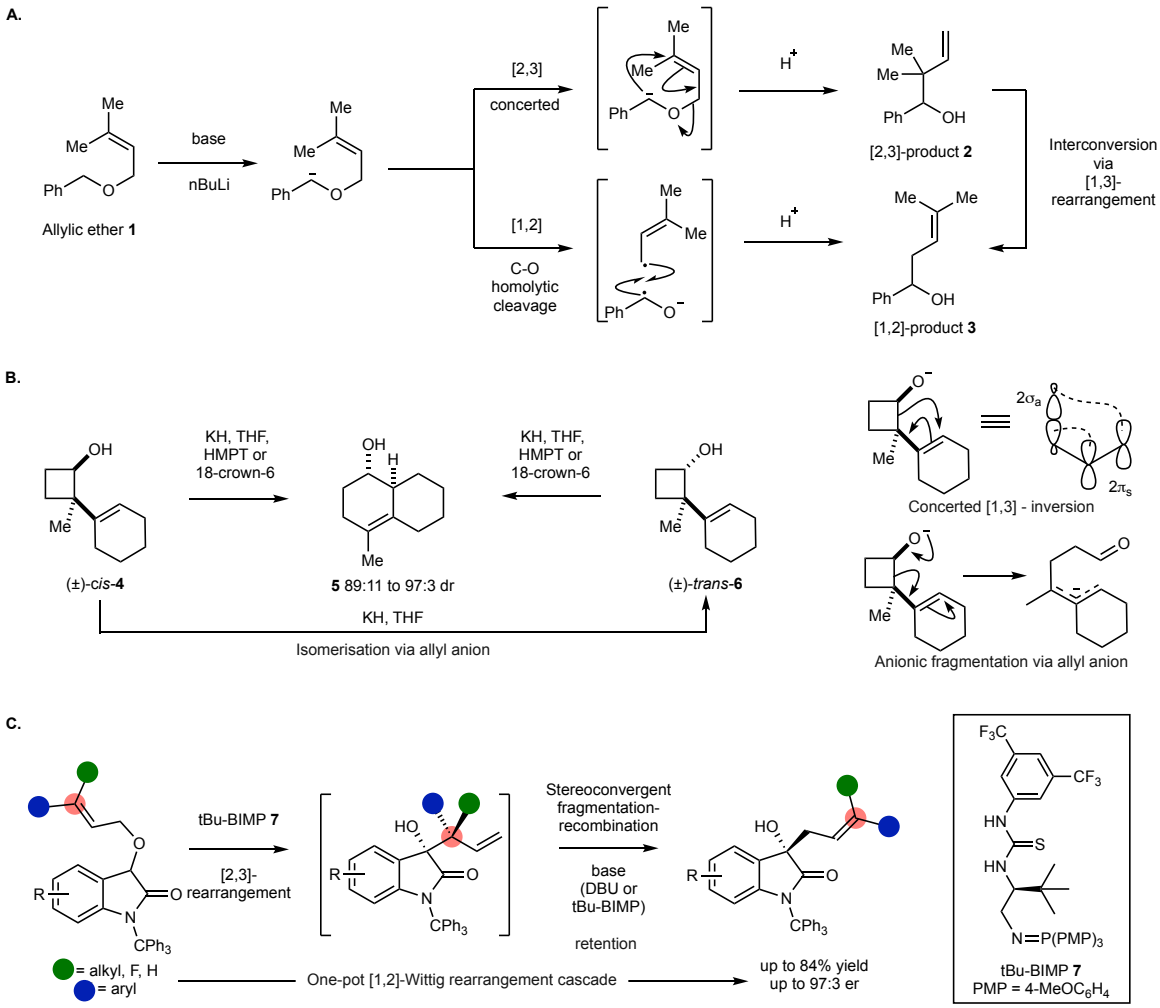

Figure 1: Overview of [2,3]-, [1,2]- and [1,3]-rearrangement pathways. **A.** Traditional mechanism and dichotomy between [2,3]- and [1,2]-Wittig rearrangements. **B.** Stereochemical ambiguity of [1,3]-rearrangement reactions *via* concerted or fragmentary pathways. **C.** This work: the catalytic enantioselective [1,2]-Wittig rearrangement cascade.

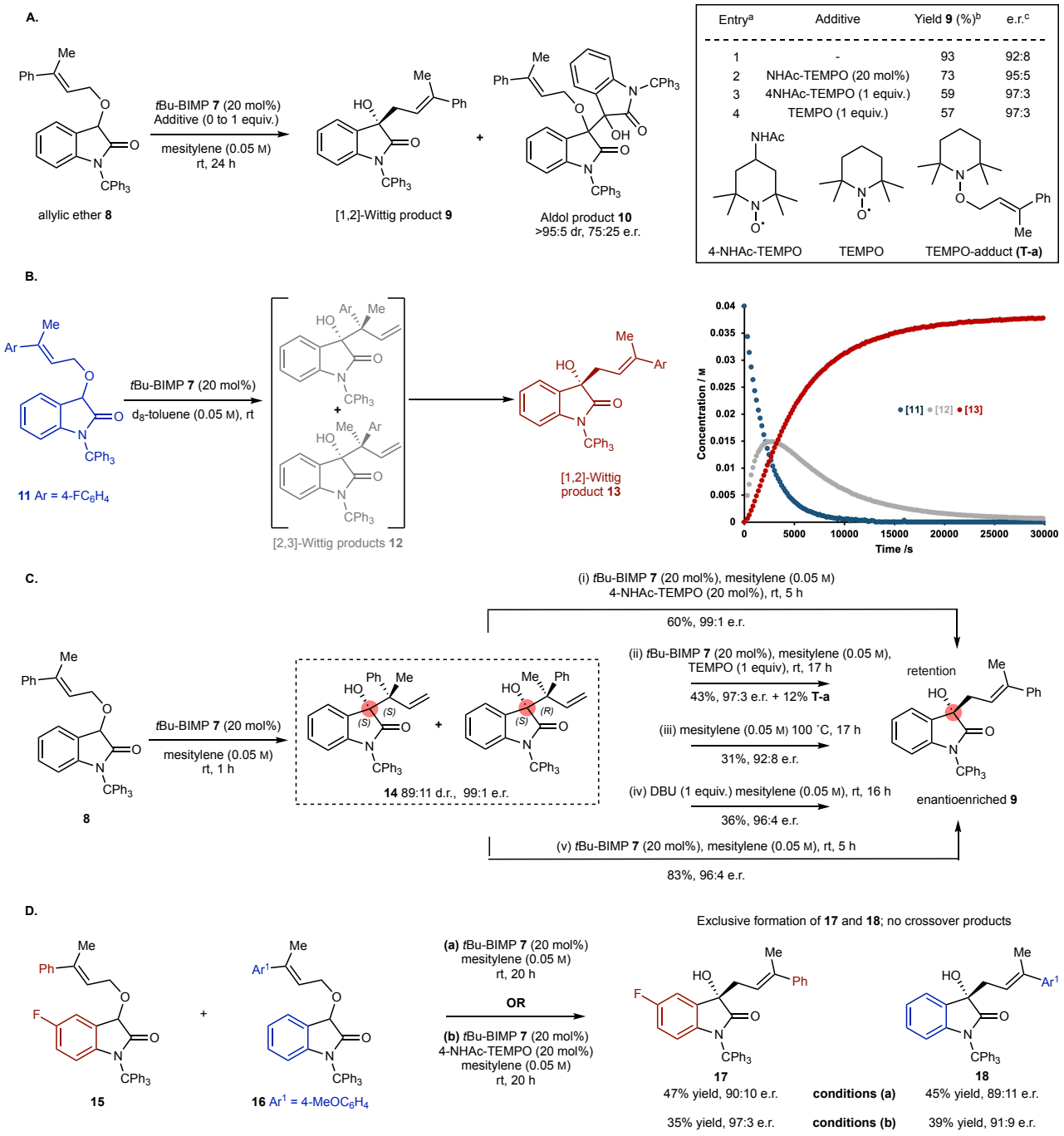

Figure 2: Demonstration of [1,2]-Wittig cascade and intermediate validation. **A.** Initial observations of [1,2]-Wittig reaction products and additive effect. [a] Reaction performed on 0.1 mmol scale. [b] all yields are isolated. [c] Determined by HPLC analysis on a chiral stationary phase. **B.** *In situ* reaction monitoring of [1,2]-Wittig cascade by ^{1}H NMR spectroscopy. [**12**] refers to combined concentration of two diastereoisomers. **C.** Control experiments validate [2,3]-Wittig products as intermediates in cascade. **D.** Crossover experiments indicate an intramolecular rearrangement process.

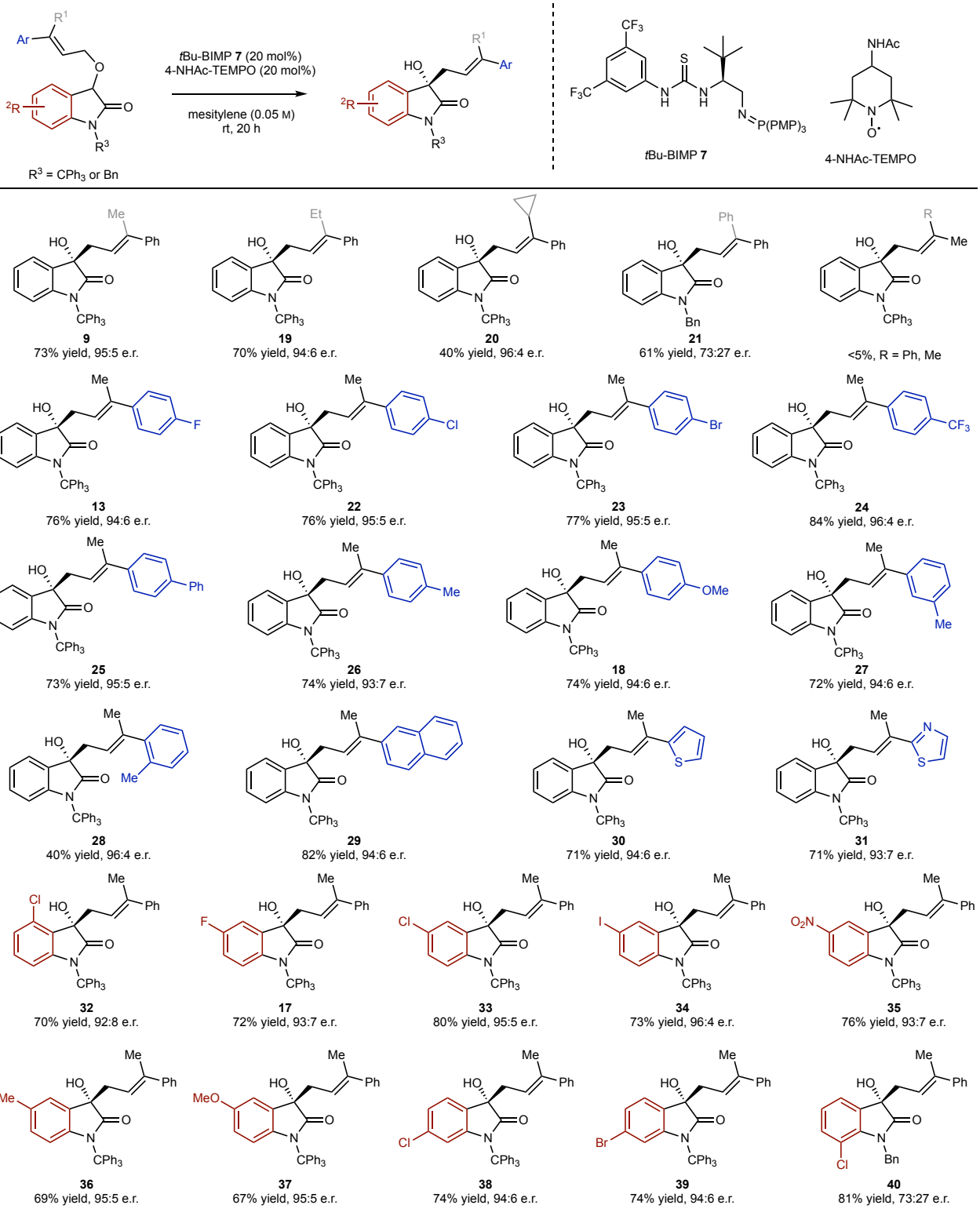

Table 1: Substrate scope and limitations of the [1,2]-Wittig rearrangement cascade; all e.r.s determined by HPLC analysis on a chiral stationary phase; all yields are isolated yields.

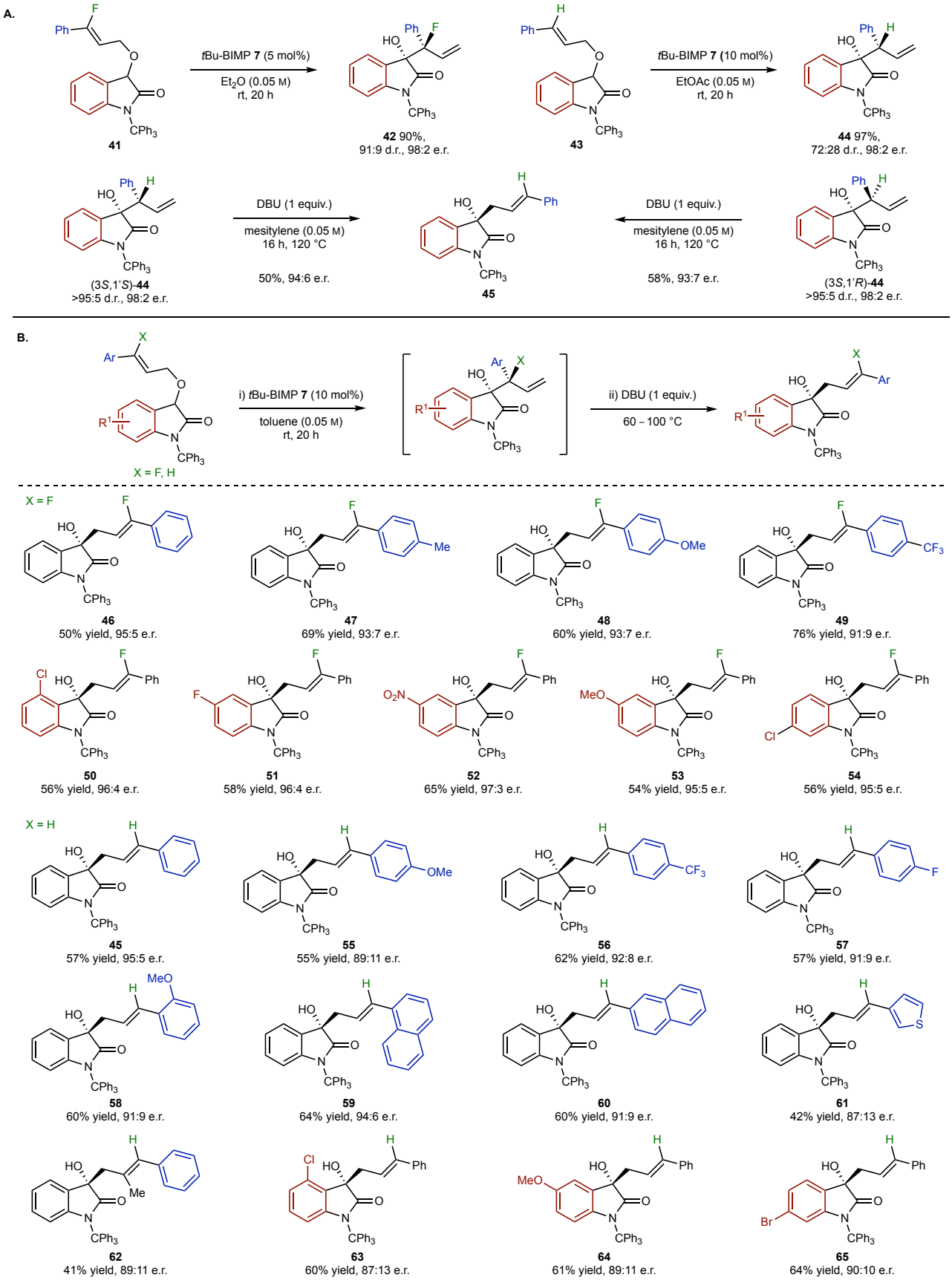

Figure 3: Effect of C(3)-substitution on [2,3]- and [1,2]-reaction pathways. **A.** Observations with C(3')-F or C(3')-H substitution; selective formation of [2,3]-rearrangement product and temperature required to promote [1,3]-rearrangement. **B.** Substrate scope and limitations of the telescoped [1,2]-Wittig process; all e.r.s

determined by HPLC analysis on a chiral stationary phase; all yields are isolated yields; *t*Bu-BIMP **7** (20 mol %) used to prepare **62**.

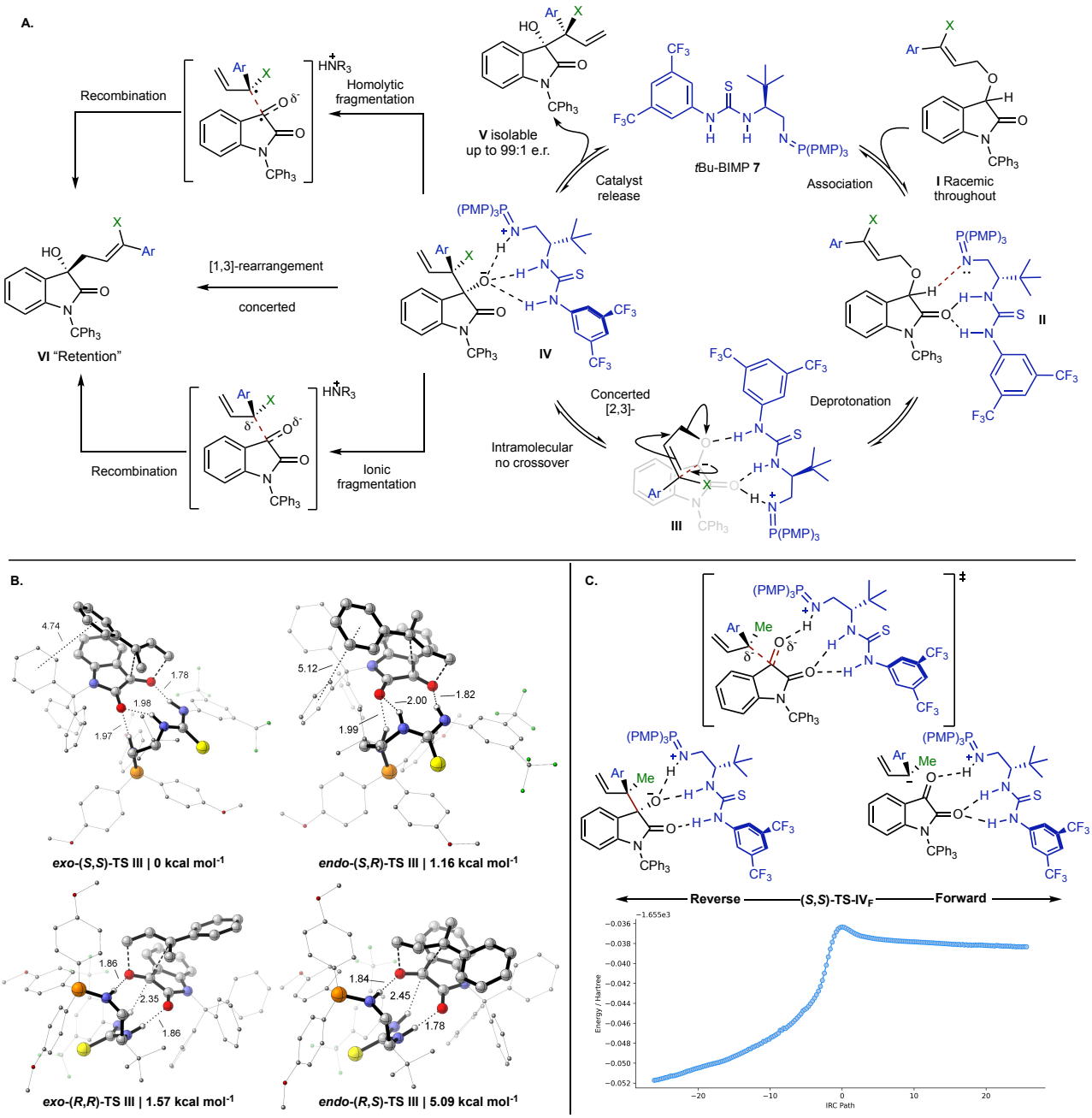

Figure 4: Catalytic cycle and computational analysis. **A**. Plausible mechanisms considered for the [1,2]-Wittig cascade. **B.** Lowest energy [2,3]-rearrangement TSs (M06-2X/Def2-TZVPP/IEFPCM(mesitylene)//ONIOM(M06-2X/6-31+G(d):AM1)) leading to the formation of the 4 possible stereoisomers; images were created in CYLview20[63]. Relative free energies are listed below each structure. **C.** IRC plot for the [1,3]-fragmentation TS **(*S*,*S*)-TS IV$_F$** (ONIOM(M06-2X/6-31+G(d):AM1)), (Ar = 4-FC_6H_4).

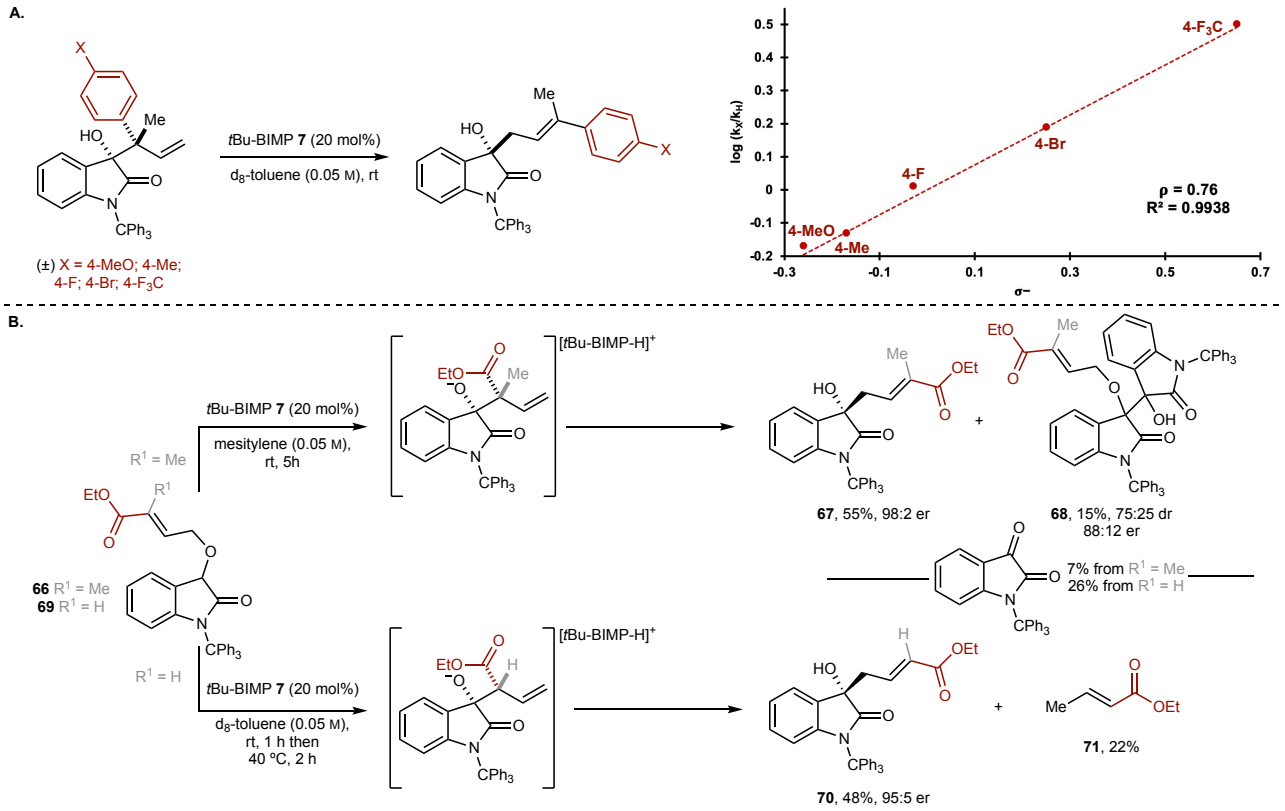

Figure 5: Mechanistic experiments. **A.** Hammett analysis of the [1,3]-rearrangement. **B.** Effect of anion stabilising ester substituents.

References:

1 Woodward, R. B. & Hoffmann, R. The Conservation of Orbital Symmetry. *Angew. Chem. Int. Ed.* **8**, 781-853 (1969).

2 J. Zeh, M. H. in *Stereoselective Synthesis* Ch. 3.7, 347-382 (2011).

3 Nakai, T. & Mikami, K. [2,3]-Wittig sigmatropic rearrangements in organic synthesis. *Chem. Rev.* **86**, 885-902 (1986).

4 Minoru Isobe, C. P. in *Molecular Rearrangements in Organic Synthesis* (ed Christian M. Rojas) 539-568 (2015).

5 Baldwin, J. E. & Patrick, J. E. Stereochemistry of [2,3]-sigmatropic reactions. Wittig rearrangement. *J. Am. Chem. Soc.* **93**, 3556-3558 (1971).

6 Nakai, T. & Mikami, K. in *Organic Reactions* 105-209 (2004).

7 Rautenstrauch, V. The Wittig rearrangement of some allyl ethers. *J. Chem. Soc. D: Chem. Commun.*, 4-6 (1970).

8 Baldwin, J. E., DeBernardis, J. & Patrick, J. E. Anion rearrangements: duality of mechanism in the decomposition of allylic ether anions and synthetic applications. *Tetrahedron Lett.* **11**, 353-356 (1970).

9 Cookson, R. C. & Kemp, J. E. Retention of configuration at the migrating centre in both photochemical and thermal [1,3]-sigmatropic shift of a benzyl group. Relaxation of orbital symmetry control in an unsymmetrical allyl system. *J. Chem. Soc. D: Chem. Commun.*, 385-386 (1971).

10 Yamamoto, Y., Oda, J. i. & Inouye, Y. The Wittig rearrangement of fluorenyl ethers in two-phase system. *Tetrahedron Lett.* **20**, 2411-2414 (1979).

11 Jemison, R. W., Ollis, W. D., Sutherland, I. O. & Tannock, J. Base catalysed rearrangements involving ylide intermediates. Part 4. [1,3] Sigmatropic rearrangements of 4-dimethylaminobutenes and [3,3] sigmatropic rearrangements of 3-dimethylaminohexa-1,5-dienes. *J. Chem. Soc. Perkin Trans. 1*, 1462-1472 (1980).

12 Wilson, S. R. in *Organic Reactions* 93-250 (2004).

13 Denmark, S. E. & Cullen, L. R. Development of a Phase-Transfer-Catalyzed, [2,3]-Wittig Rearrangement. *J. Org. Chem.* **80**, 11818-11848 (2015).

14 Kennedy, C. R., Guidera, J. A. & Jacobsen, E. N. Synergistic Ion-Binding Catalysis Demonstrated via an Enantioselective, Catalytic [2,3]-Wittig Rearrangement. *ACS Cent. Sci.* **2**, 416-423 (2016).

15 Zhao, L.-M., Zhang, A.-L., Zhang, J.-H., Gao, H.-S. & Zhou, W. Zinc-Mediated C-3 α-Prenylation of Isatins with Prenyl Bromide: Access to 3-Prenyl-3-hydroxy-2-oxindoles and Its Application. *J. Org. Chem.* **81**, 5487-5494 (2016).
16 Danheiser, R. L., Martinez-Davila, C. & Sard, H. Cyclohexenol annulation via the alkoxy-accelerated rearrangement of vinylcyclobutanes. *Tetrahedron* **37**, 3943-3950 (1981).
17 Harris, N. J. & Gajewski, J. J. Mechanism of the 1,3-Sigmatropic Shift of 2-Vinylcyclobutanol Alkoxides. *J. Am. Chem. Soc.* **116**, 6121-6129 (1994).
18 Bhupathy, M. & Cohen, T. Control of stereochemistry in potassium alkoxide accelerated [1,3] sigmatropic rearrangements by the use of a crown ether for the apparent destruction of ion pairs. Evidence for a fragmentation mechanism in a vinylcyclobutane rearrangement. *J. Am. Chem. Soc.* **105**, 6978-6979 (1983).
19 Kim, S.-H., Cho, S. Y. & Cha, J. K. On the stereochemistry of anion-accelerated [1,3]-sigmatropic rearrangement of 2-vinylcyclobutanols. *Tetrahedron Lett.* **42**, 8769-8772 (2001).
20 Chogii, I., Das, P., Fell, J. S., Scott, K. A., Crawford, M. N., Houk, K. N. & Njardarson, J. T. New Class of Anion-Accelerated Amino-Cope Rearrangements as Gateway to Diverse Chiral Structures. *J. Am. Chem. Soc.* **139**, 13141-13146 (2017).
21 Spules, T. J., Galpin, J. D. & Macdonald, D. Charge-accelerated cope rearrangements of 3-amino-1,5-dienes. *Tetrahedron Lett.* **34**, 247-250 (1993).
22 Dobson, H. K., LeBlanc, R., Perrier, H., Stephenson, C., Welch, T. R. & Macdonald, D. [1,3] and [3,3] rearrangements of 3-amino-1,5-hexadienes: Solvent effect on the regioselectivity. *Tetrahedron Lett.* **40**, 3119-3122 (1999).
23 Tomooka, K., Yamamoto, K. & Nakai, T. Enantioselective [1,2] Wittig Rearrangement Using an External Chiral Ligand. *Angew. Chem. Int. Ed.* **38**, 3741-3743 (1999).
24 Zieger, H. E., Bright, D. A. & Haubenstock, H. Syntheses of .alpha.-phenylneopentyl chloride enantiomers: (S)-(-)-1-chloro-1-phenyl-2,2-dimethylpropane from (R)-(+)-1-phenyl-2,2-dimethyl-1-propanol via the reaction of tri-n-butylphosphine in carbon tetrachloride and (R)-(+)-1-chloro-1-phenyl-2,2-dimethylpropane from anthranilic acid. *J. Org. Chem.* **51**, 1180-1184 (1986).
25 Iglesias-Fernández, J., Hancock, S. M., Lee, S. S., Khan, M., Kirkpatrick, J., Oldham, N. J., McAuley, K., Fordham-Skelton, A., Rovira, C. & Davis, B. G. A front-face 'SNi synthase' engineered from a retaining 'double-SN2' hydrolase. *Nat. Chem. Biol.* **13**, 874-881 (2017).
26 Paparella, A. S., Cahill, S. M., Aboulache, B. L. & Schramm, V. L. Clostridioides difficile TcdB Toxin Glucosylates Rho GTPase by an SNi Mechanism and Ion Pair Transition State. *ACS Chem. Biol.* **17**, 2507-2518 (2022).
27 Pronin, S. V., Reiher, C. A. & Shenvi, R. A. Stereoinversion of tertiary alcohols to tertiary-alkyl isonitriles and amines. *Nature* **501**, 195-199 (2013).
28 Marcyk, P. T., Jefferies, L. R., AbuSalim, D. I., Pink, M., Baik, M.-H. & Cook, S. P. Stereoinversion of Unactivated Alcohols by Tethered Sulfonamides. *Angew. Chem. Int. Ed.* **58**, 1727-1731 (2019).
29 Watile, R. A., Bunrit, A., Margalef, J., Akkarasamiyo, S., Ayub, R., Lagerspets, E., Biswas, S., Repo, T. & Samec, J. S. M. Intramolecular substitutions of secondary and tertiary alcohols with chirality transfer by an iron(III) catalyst. *Nat. Commun.* **10**, 3826 (2019).
30 Lanke, V. & Marek, I. Stereospecific nucleophilic substitution at tertiary and quaternary stereocentres. *Chem. Sci.* **11**, 9378-9385 (2020).
31 Lanke, V. & Marek, I. Nucleophilic Substitution at Quaternary Carbon Stereocenters. *J. Am. Chem. Soc.* **142**, 5543-5548 (2020).
32 Zhang, X. & Tan, C.-H. Stereospecific and stereoconvergent nucleophilic substitution reactions at tertiary carbon centers. *Chem* **7**, 1451-1486 (2021).
33 Formica, M., Rozsar, D., Su, G., Farley, A. J. M. & Dixon, D. J. Bifunctional Iminophosphorane Superbase Catalysis: Applications in Organic Synthesis. *Acc. Chem. Res.* **53**, 2235-2247 (2020).
34 Bray, J. M., Stephens, S. M., Weierbach, S. M., Vargas, K. & Lambert, K. M. Recent Advancements in the Use of Bobbitt's Salt and 4-AcetamidoTEMPO. *Chem. Commun.* (2023).
35 Griller, D., Ingold, K. U. *Acc. Chem. Res.* 13, 317-323 (1980).
36 Steigerwald, M. L., Goddard, W. A., III & Evans, D. A. Theoretical studies of the oxy anionic substituent effect. *J. Am. Chem. Soc.* **101**, 1994-1997 (1979).
37 Grimme, S., Bohle, F., Hansen, A., Pracht, P., Spicher, S. & Stahn, M. Efficient Quantum Chemical Calculation of Structure Ensembles and Free Energies for Nonrigid Molecules. *J. Phys. Chem. A* **125**, 4039-4054 (2021).

38 Pracht, P., Bohle, F. & Grimme, S. Automated exploration of the low-energy chemical space with fast quantum chemical methods. *Phys. Chem. Chem. Phys.* **22**, 7169-7192 (2020).
39 Pracht, P., Grimme, S., Bannwarth, C., Bohle, F., Ehlert, S., Feldmann, G., Gorges, J., Müller, M., Neudecker, T., Plett, C., Spicher, S., Steinbach, P., Wesołowski, P. A. & Zeller, F. CREST—A program for the exploration of low-energy molecular chemical space. *J. Chem. Phys.* **160** (2024).
40 Gaussian 16 Revision C.01, Frisch, M. J., Trucks, G. W., Schlegel, H. B., Scuseria, G. E., Robb, M. A., Cheeseman, J. R., Scalmani, G., Barone, V., Petersson, G. A., Nakatsuji, H., Li, X., Caricato, M., Marenich, A. V., Bloino, J., Janesko, B. G., Gomperts, R., Mennucci, B., Hratchian, H. P., Ortiz, J. V., Izmaylov, A. F., Sonnenberg, J. L., Williams-Young, D., Ding, F., Lipparini, F., Egidi, F., Goings, J., Peng, B., Petrone, A., Henderson, T., Ranasinghe, D., Zakrzewski, V. G., Gao, J., Rega, N., Zheng, G., Liang, W., Hada, M., Ehara, M., Toyota, K., Fukuda, R., Hasegawa, J., Ishida, M., Nakajima, T., Honda, Y., Kitao, O., Nakai, H., Vreven, T., Throssell, K., Montgomery Jr., J. A., Peralta, J. E., Ogliaro, F., Bearpark, M. J., Heyd, J. J., Brothers, E. N., Kudin, K. N., Staroverov, V. N., Keith, T. A., Kobayashi, R., Normand, J., Raghavachari, K., Rendell, A. P., Burant, J. C., Iyengar, S. S., Tomasi, J., Cossi, M., Millam, J. M., Klene, M., Adamo, C., Cammi, R., Ochterski, J. W., Martin, R. L., Morokuma, K., Farkas, O., Foresman, J. B. & Fox, D. J. Gaussian, Inc., Wallingford, CT, 2016.
41 Svensson, M., Humbel, S., Froese, R. D. J., Matsubara, T., Sieber, S. & Morokuma, K. ONIOM: A Multilayered Integrated MO + MM Method for Geometry Optimizations and Single Point Energy Predictions. A Test for Diels−Alder Reactions and Pt(P(t-Bu)3)2 + H2 Oxidative Addition. *J. Phys. Chem.* **100**, 19357-19363 (1996).
42 Chung, L. W., Sameera, W. M. C., Ramozzi, R., Page, A. J., Hatanaka, M., Petrova, G. P., Harris, T. V., Li, X., Ke, Z., Liu, F., Li, H.-B., Ding, L. & Morokuma, K. The ONIOM Method and Its Applications. *Chem. Rev.* **115**, 5678-5796 (2015).
43 Grayson, M. N., Pellegrinet, S. C. & Goodman, J. M. Mechanistic Insights into the BINOL-Derived Phosphoric Acid-Catalyzed Asymmetric Allylboration of Aldehydes. *J. Am. Chem. Soc.* **134**, 2716-2722 (2012).
44 Lam, C. C. & Goodman, J. M. Computational insights on the origin of enantioselectivity in reactions with diarylprolinol silyl ether catalysts via a radical pathway. *Org. Chem. Front.* **9**, 3730-3738 (2022).
45 Simón, L. Enantioselectivity in CPA-catalyzed Friedel–Crafts reaction of indole and N-tosylimines: a challenge for guiding models. *Org. Biolmol. Chem.* **16**, 2225-2238 (2018).
46 Simón, L. & Goodman, J. M. Theoretical Study of the Mechanism of Hantzsch Ester Hydrogenation of Imines Catalyzed by Chiral BINOL-Phosphoric Acids. *J. Am. Chem. Soc.* **130**, 8741-8747 (2008).
47 Simón, L. & Goodman, J. M. Mechanism of BINOL−Phosphoric Acid-Catalyzed Strecker Reaction of Benzyl Imines. *J. Am. Chem. Soc.* **131**, 4070-4077 (2009).
48 Simón, L. & Goodman, J. M. What is the mechanism of amine conjugate additions to pyrazole crotonate catalyzed by thiourea catalysts? *Org. Biolmol. Chem.* **7**, 483-487 (2009).
49 Simón, L. & Goodman, J. M. A Model for the Enantioselectivity of Imine Reactions Catalyzed by BINOL−Phosphoric Acid Catalysts. *J. Org. Chem.* **76**, 1775-1788 (2011).
50 Peng, Q., Duarte, F. & Paton, R. S. Computing organic stereoselectivity – from concepts to quantitative calculations and predictions. *Chem. Soc. Rev.* **45**, 6093-6107 (2016).
51 Huber, R. G., Margreiter, M. A., Fuchs, J. E., von Grafenstein, S., Tautermann, C. S., Liedl, K. R. & Fox, T. Heteroaromatic π-Stacking Energy Landscapes. *J. Chem. Inf. Model.* **54**, 1371-1379 (2014).
52 Berson, J. A. & Nelson, G. L. Inversion of configuration in the migrating group of a thermal 1,3-sigmatropic rearrangement. *J. Am. Chem. Soc.* **89**, 5503-5504 (1967).
53 Bernardi, F., Olivucci, M., Robb, M. A. & Tonachini, G. Can a photochemical reaction be concerted? A theoretical study of the photochemical sigmatropic rearrangement of but-1-ene. *J. Am. Chem. Soc.* **114**, 5805-5812 (1992).
54 Wilsey, S. & Houk, K. N. H/Allyl and Alkyl/Allyl Conical Intersections: Ubiquitous Control Elements in Photochemical Sigmatropic Shifts. *J. Am. Chem. Soc.* **122**, 2651-2652 (2000).
55 Houk, K. N., Li, Y. & Evanseck, J. D. Transition Structures of Hydrocarbon Pericyclic Reactions. *Angew. Chem. Int. Ed.* **31**, 682-708 (1992).
56 Ascough, D. M. H., Duarte, F. & Paton, R. S. Stereospecific 1,3-H Transfer of Indenols Proceeds via Persistent Ion-Pairs Anchored by NH···π Interactions. *J. Am. Chem. Soc.* **140**, 16740-16748 (2018).
57 Hammer, N., Christensen, M. L., Chen, Y., Naharro, D., Liu, F., Jørgensen, K. A. & Houk, K. N. An Experimental Stereoselective Photochemical [1s,3s]-Sigmatropic Silyl Shift and the Existence of Silyl/Allyl Conical Intersections. *J. Am. Chem. Soc.* **142**, 6030-6035 (2020).

58 Mita, T., Takano, H., Hayashi, H., Kanna, W., Harabuchi, Y., Houk, K. N. & Maeda, S. Prediction of High-Yielding Single-Step or Cascade Pericyclic Reactions for the Synthesis of Complex Synthetic Targets. *J. Am. Chem. Soc.* **144**, 22985-23000 (2022).
59 Vogler, T. & Studer, A. Applications of TEMPO in Synthesis. *Synthesis* **2008**, 1979-1993 (2008).
60 Leifert, D. & Studer, A. Organic Synthesis Using Nitroxides. *Chem. Rev.* **123**, 10302-10380 (2023).
61 Whitesides, G. M. & Newirth, T. L. Reaction of n-butyllithium and 2,2,6,6-tetramethylpiperidine nitroxyl. *J. Org. Chem.* **40**, 3448-3450 (1975).
62 Nagashima, T. & Curran, D. P. Reactions of Tempo with Alkylsamarium and Other Organometallic Reagents. *Synlett* **1996**, 330-332 (1996).
63 CYLview20 Legault, C., Université de Sherbrooke, 2020.

Methods:

Typical procedures for the [1,2]-rearrangement cascade at room temperature and upon heating are exemplified below.

Procedure for BIMP-catalyzed enantioselective [1,2]-rearrangement reaction at room temperature: reaction and purification to give 9

The allylic ether substrate **8** (52.1 mg, 0.1 mmol), *t*Bu-BIMP **7** (14.7 mg, 0.02 mmol) and 4-NHAc-TEMPO (4.3 mg, 0.02 mmol) were added to a flame-dried Schlenk tube and the tube was flushed with N_2 three times. Mesitylene (2 mL, 0.05 M) was added through the septum under a positive pressure of N_2. The reaction was stirred at rt for 16 h until completion as indicated by TLC analysis. The reaction mixture was concentrated under reduced pressure to give the crude product, which was purified by flash column chromatography (silica gel: eluent hexane/ EtOAc = 4:1 → 3:1) to afford **9** (38.0 mg, 73%) as a colourless amorphous solid. The e.r. was obtained by high-performance liquid chromatography (chiral stationary phase) of the purified products (Daicel CHIRALCEL ODH column (10% *i*-PrOH in hexane; 1.0 ml min^{-1}; T = 30 °C; 211 nm); retention time (minor) = 7.0 min, retention time (major) =8.7 min; 5:95 e.r.).

Procedure for BIMP-catalyzed enantioselective [1,2]-rearrangement reaction cascade involving heating with DBU: reaction, work-up and purification to give 45

The allylic ether substrate **43** (101.5mg, 1.0 equiv.) and *t*Bu-BIMP **7** (14.8mg, 10 mol%) were added to a vial before the addition of toluene (4 mL, 0.05 M). The mixture was stirred at rt for 24 h, then DBU (28 µL, 1.0 equiv.) was added, and the mixture was then heated to 100 °C and stirred for 16 h, then quenched by addition of sat. aq. NH4Cl and diluted with EtOAc. The phases were separated, and the aqueous phase was extracted with EtOAc (×2). The combined organic phases were washed with brine, dried ($MgSO_4$) and concentrated under reduced pressure. The residue was purified by flash column chromatography (silica gel: eluent 80:20 → 75:25 petrol/EtOAc) to afford **45** (58 mg, 57%) as a yellow amorphous solid. The e.r. was obtained by high-performance liquid chromatography (chiral stationary phase) of the purified products (Daicel CHIRALPAK ADH column (10% *i*-PrOH in hexane; 1.0 ml min^{-1}; T = 30 °C; 211 nm); retention time (minor) = 12.5 min, retention time (major) =14.6 min; 5:95 e.r.).

Data availability:

Data are available in the manuscript and supplementary materials. The research data supporting this publication can be accessed at https://doi.org/10.17630/5b5778a0-f337-4cbe-b336-c2afac22693b and https://doi.org/10.17630/6424d442-e1bc-4834-9456-6cfb7296580f: data underpinning "The Catalytic Enantioselective [1,2]-Wittig Rearrangement Cascade of Allylic Ethers". University of St Andrews Research Portal; PURE ID: 295983644 and 320215223. Gaussian files plus three sets of in situ reaction monitoring data and a Python script which fits the rate constants of a first-order kinetics model to the experimental data are openly available in Dataset for "The Catalytic Enantioselective [1,2]-Wittig Rearrangement Cascade of Allylic Ethers" in the University of Bath Research Data Archive at https://doi.org/10.15125/BATH-01337. The supplementary crystallographic data for this paper are available free of charge from the Cambridge Crystallographic Data Centre (CCDC) under accession numbers 2305636 (for compound **S24**) and 2305637 (for compound **S25**).

Authors and Affiliations:
EaStCHEM, School of Chemistry, University of St Andrews, North Haugh, St Andrews, KY16 9ST, UK.
Tengfei Kang, Justin O'Yang, Kevin Kasten, Martin Juhl, David B. Cordes, Aidan P. McKay, Andrew D. Smith
Key Laboratory of Applied Surface and Colloid Chemistry, Ministry of Education, and School of Chemistry and Chemical Engineering, Shaanxi Normal University, Xi'an, Shaanxi, China, 710119.
Tengfei Kang
Department of Chemistry, University of Bath, Claverton Down, Bath, BA2 7AY, UK.
Samuel S. Allsop, Toby Lewis-Atwell, Elliot H. E. Farrar, Matthew N. Grayson
Department of Computer Science, University of Bath, Claverton Down, Bath, BA2 7AY, UK.
Toby Lewis-Atwell

Corresponding Authors:
Correspondence to **ADS** (ads10@st-andrews.ac.uk) and **MNG** (M.N.Grayson@bath.ac.uk)